ARTICLE

Genetic control of the human brain proteome

Chloe Robins,[1] Yue Liu,[1] Wen Fan,[1] Duc M. Duong,[2] Jacob Meigs,[1] Nadia V. Harerimana,[1] Ekaterina S. Gerasimov,[1] Eric B. Dammer,[2] David J. Cutler,[3] Thomas G. Beach,[4] Eric M. Reiman,[5] Philip L. De Jager,[7] David A. Bennett,[8] James J. Lah,[1] Aliza P. Wingo,[9,10] Allan I. Levey,[1] Nicholas T. Seyfried,[2,*] and Thomas S. Wingo[1,3,*]

Summary

We generated an online brain pQTL resource for 7,376 proteins through the analysis of genetic and proteomic data derived from post-mortem samples of the dorsolateral prefrontal cortex of 330 older adults. The identified pQTLs tend to be non-synonymous variation, are over-represented among variants associated with brain diseases, and replicate well (77%) in an independent brain dataset. Comparison to a large study of brain eQTLs revealed that about 75% of pQTLs are also eQTLs. In contrast, about 40% of eQTLs were identified as pQTLs. These results are consistent with lower pQTL mapping power and greater evolutionary constraint on protein abundance. The latter is additionally supported by observations of pQTLs with large effects' tending to be rare, deleterious, and associated with proteins that have evidence for fewer protein-protein interactions. Mediation analyses using matched transcriptomic and proteomic data provided additional evidence that pQTL effects are often, but not always, mediated by mRNA. Specifically, we identified roughly 1.6 times more mRNA-mediated pQTLs than mRNA-independent pQTLs (550 versus 341). Our pQTL resource provides insight into the functional consequences of genetic variation in the human brain and a basis for novel investigations of genetics and disease.

Introduction

Analyses mapping expression quantitative trait loci (eQTLs) have deepened our understanding of the links between genetics and disease.[1–5] eQTLs tend to overlap with disease-associated variants identified by genome-wide association studies (GWASs) and are often used to provide insight into the functional consequences of genetic variation and identify candidate causal genes.[6–10] These investigations implicitly assume that the genetic effects on mRNA expression propagate to protein—the main determinant of cellular function and ultimately most phenotypes. However, gene expression is not a perfect proxy for protein expression. Previous studies have shown that mRNA and protein abundances are often only weakly correlated.[11,12] Furthermore, analyses mapping protein quantitative trait loci (pQTLs), in addition to eQTLs, have shown pQTLs to provide novel insight into the impacts of genetic variation.[13–18] Since proteins represent a major source of druggable molecular targets, this information can greatly aid the development of new therapeutics.[19]

The genetic control of mRNA expression in the brain has been well studied,[20–27] but currently little is known about how genetics influences brain protein abundances. Large-scale analyses of brain pQTLs have not yet been performed because the necessary data have only recently emerged. Here, we investigate the genetic control of the human brain proteome by using high-throughput mass spectrometry-based protein data from post-mortem brain samples of the dorsolateral prefrontal cortex (dPFC) of older adults. Additionally, to better understand the relationship between the genetic control of the human brain proteome and transcriptome, we compare the pQTL results to a recent brain eQTL meta-analysis and perform mediation analyses by using matched gene and protein expression data. The results of our pQTL analyses are made available on the pQTL web application as a resource for future investigations (see "Web resources").

Material and methods

Data

Discovery dataset

To investigate the genetic control of the human brain proteome, we analyzed genetic, transcriptomic, and proteomic data derived from post-mortem samples of the dPFC of participants of the Religious Orders Study (ROS) and Rush Memory and Aging Project (MAP).[28–30] ROS and MAP are longitudinal cohort studies of aging and dementia maintained by investigators at the Rush Alzheimer Disease Center in Chicago, IL.[28–30] Both studies recruit participants without known dementia at baseline and follow them annually via detailed clinical evaluation. The studies were approved by an institutional review board of Rush University Medical Center. All participants provided informed consent and signed an Anatomic Gift Act and repository consent to allow their data and biospecimens to be repurposed.

[1]Department of Neurology, Emory University School of Medicine, Atlanta, GA 30322, USA; [2]Department of Biochemistry, Emory University School of Medicine, Atlanta, GA 30322, USA; [3]Department of Human Genetics, Emory University School of Medicine, Atlanta, GA 30322, USA; [4]Banner Sun Health Research Institute, Sun City, AZ 85351, USA; [5]Banner Alzheimer's Institute, Arizona State University and University of Arizona, Phoenix, AZ 85351, USA; [7]Center for Translational and Computational Neuroimmunology, Department of Neurology, Columbia University Medical Center, New York, NY 10032, USA; [8]Rush Alzheimer Disease Center, Rush University Medical Center, Chicago, IL 60612, USA; [9]Division of Mental Health, Atlanta VA Medical Center, Decatur, GA 30033, USA; [10]Department of Psychiatry, Emory University School of Medicine, Atlanta, GA 30322, USA

*Correspondence: thomas.wingo@emory.edu (T.S.W.), nseyfri@emory.edu (N.T.S.)

https://doi.org/10.1016/j.ajhg.2021.01.012.

Proteomic data. Protein abundance data from cortical microdissections of the dPFC of ROS/MAP subjects were generated via tandem mass tag (TMT) isobaric labeling mass spectrometry methods for protein identification and quantification, as previously described by Johnson et al. (2020)[31] and Wingo et al. (2020).[32] Briefly, tissue homogenization, protein digestion, TMT labeling, and high-pH fractionation were performed in sequence. An equal amount of protein digested from each sample was aliquoted and digested in parallel to serve as the global pooled internal standard (GIS) in each TMT batch. Prior to TMT labeling, all samples were randomized into 50 batches (8 samples per batch) based on age at death, sex, post-mortem interval, diagnosis, and measured neuropathologies. Peptides from each individual sample ($n = 400$) and the GIS ($n = 100$) were labeled with the TMT 10-plex kit (Thermo Fisher). All fractions were resuspended in equal volume of loading buffer and analyzed by liquid chromatography coupled to mass spectrometry. The Orbitrap Fusion mass spectrometer (Thermo Fisher Scientific) was run with MS/MS (MS2) scans for 45 TMT batches and with the SPS-MS3 method for five TMT batches.

All raw files were analyzed via the Proteome Discoverer suite (version 2.3 Thermo Fisher Scientific). MS2 spectra were searched against the canonical UniProtKB human proteome database (downloaded February 2019 with 20,338 total sequences). The Sequest HT search engine was used and parameters were specified as previously described by Johnson et al. (2020)[31] and Wingo et al. (2020).[32] Peptide spectral matches (PSMs) and peptides were filtered with Percolator to a false discovery rate (FDR) of less than one percent. Peptides were then assembled into proteins and further filtered on the basis of the combined probabilities of the constituent peptides to a final FDR of less than one percent. In cases of redundancy, shared peptides were assigned to protein sequences in adherence with the principles of parsimony. Reporter ions were quantified from MS2 or MS3 scans via an integration tolerance of 20 ppm with the most confident centroid setting. A total of 12,691 proteins were quantified. Correlation of technical replicates within each batch was over 99%, indicating a high degree of reproducibility for the quantified proteins (Figure S1).

To ensure the analysis of high-quality data, we excluded proteins with low correlations between the two GISs (outside the 95% confidence interval) within batches and proteins with missing data for over 50% of subjects across batches. Additionally, we scaled each abundance value by a subject-specific total protein abundance measure to remove the effects of loading differences in the proteomic experiments. After transformation to the log2 scale, outlier subjects were identified and removed through iterative principal-component analysis. For each iteration, subjects more than four standard deviations from the mean of the first or second principal component were removed and the principal components were re-calculated. Following outlier removal, proteins with missing data for over 50% of the remaining subjects were removed. Finally, we residualized the abundance of each protein via linear regression to remove the effects of sex, age at death, post-mortem interval, study, batch, and MS2 versus MS3 reporter quantitation mode. After these quality control procedures, there were 7,376 high-quality proteins available for analysis.

To reduce confounding due to disease, we included dementia status at death as a covariate in all proteomic analyses. For each ROS/MAP participant, a clinical diagnosis of dementia was rendered at the time of death blinded to all pathologic data. Here, we coded the diagnoses of dementia status as no cognitive impairment (NCI), mild cognitive impairment (MCI), or Alzheimer dementia (AD) and excluded individuals with a diagnosis of non-Alzheimer dementia from analysis. For secondary analyses on the influence of disease, all described quality control procedures were repeated with data from the subset of samples with NCI at death.

Genotyping data. Genotype data were generated from whole-genome sequencing (WGS) of DNA that was extracted from cryopreserved peripheral blood mononuclear cells or frozen dPFC of ROS/MAP subjects. WGS was performed as previously described[33] and is available via Synapse (ID: syn10901595). Briefly, libraries were constructed with the KAPA Hyper Library Preparation Kit per the manufacturer's protocol and sequenced on an Illumina HiSeq X sequencer (v.2.5 chemistry) with 150 bp paired-end reads. Reads were aligned to the GRCh37 human reference genome via Burrows-Wheeler Aligner (BWA-MEM v.0.7.8)[34] and processed with the GATK best-practices workflow, which includes marking duplicate reads by Picard tools v.1.83, local realignment around indels, and base quality score recalibration by Genome Analysis Toolkit (GATK v.3.4.0).[35,36] A multi-sample genomic variant call format (gVCF) was generated by merging results of HaplotypeCaller on each sample individually in gVCF mode (GATKv.3.4.0), and batches of gVCF were merged into gVCFs processed by a joint genotyping step (GATK v.3.2.2).

Annotation of the multi-sample VCF ($n = 1,196$) was performed with Bystro.[37] After quality control, a total of 1,133 subjects remained for analysis. A total of 63 subjects were excluded for one or more of the following reasons: (1) θ, silent:replacement sites, or transition:transversion ratios greater than five standard deviations from the mean ($n = 7$); (2) genotype missingness, heterozygosity, or homozygosity greater than three standard deviations from the mean ($n = 14$); (3) sex discordance based on the heterozygosity of the X chromosome ($n = 7$); and (4) cryptic relation or duplication identified by identity-by-state sharing with PLINK[38] ($n = 31$). We used unlinked ancestrally informative markers to infer eigenvectors for principal-component analysis by using EIGENSTRAT[39] and over six standard deviation outliers ($n = 1$) were removed. Before analysis, the data was restricted to subjects of European descent and filtered to the HapMap 3 SNVs[40] that are in Hardy-Weinberg equilibrium (HWE) and have a minor allele frequency (MAF) greater than 0.05.

After quality control, we had 501,414 common SNVs to test and 330 subjects with both proteomic and genetic data. Information on the demographics and disease status of these subjects is provided in Table S1. As a result of the batch-specific nature of missing data from TMT-labeled MS/MS protein quantification, the number of subjects with proteomic data differs for each protein and ranges from 161 to 330 (Figure S2). As expected, proteins that were more abundant were also more likely to have complete data (Figure S3).

Transcriptomic data. Gene expression was measured from the dPFC as previously described.[33] Briefly, RNA was extracted from cortically dissected sections of dPFC gray matter and samples with RNA integrity numbers (RINs) over 5 were used to prepare RNA-sequencing (RNA-seq) libraries via strand-specific dUTP method with poly-A selection[41,42] with the Illumina HiSeq with 101-bp paired-end reads to a target coverage of 50 million reads per library. Raw RNA-seq reads were aligned to a GRCh38 reference genome, and gene counts were computed via STAR[43] as described in Logsdon et al. (2019).[44] We obtained RNA-seq data from Synapse (ID: syn17010685) and performed library normalization and quality control as described by Sieberts et al. (2020).[22] Genes with <1 cpm in over 50% of subjects were removed, and the remaining genes were normalized via conditional quantile normalization[45] followed by weighted normalization via the voom-lima package in Bioconductor.[46] Outlier subjects were detected and removed via principal-component analysis and hierarchical clustering. Only samples within three standard deviations of the mean of the first and second principal components were retained for further analysis. Finally, we residualized the expression of each gene via linear regression to remove the effects of sex, age at death, post-mortem interval, study, and batch. After quality control, 173 subjects had matched transcriptomic, proteomic, and genetic data. Table S1 provides the demographic and disease characteristics of these subjects.

Replication dataset

Genetic and proteomic data derived from dPFC of participants of the Banner Sun Health Brain and Body Donation Program (Banner BBDP) were used for replication analyses. The Banner Sun Health Research Institute recruited cognitively normal individuals from the retirement communities of the greater Phoenix, AZ.[47] The study was approved by the Banner Sun Health Research Institute Institutional Review Board, and all individuals or their legal representatives provided informed consent for participation.

Proteomic data. Proteomic profiling was performed with the samples of the dPFC following the same approach as described for ROS/MAP subjects with two differences: (1) only MS2 scans were obtained and (2) MS2 spectra were searched against the UniProtKB human brain proteome database downloaded in April 2015. A total of 11,518 proteins were quantified. We used the same quality control procedures as the ROS/MAP proteomic data to remove proteins with more than 50% missing data, remove outlier individuals, and remove the effects covariates (i.e., age at death, sex, batch, and post-mortem interval) from the proteomic profiles. After these quality control procedures, there were 6,526 high-quality proteins available for analysis.

Analogous to the analyses in the discovery dataset, dementia status at death was included as in all relevant models. Banner BBDP participants were assessed during life with annual medical, neurologic, and neuropsychological assessments, and upon death, their donated brains underwent detailed neuropathologic assessment. The final clinical diagnoses of Banner BBDP participants was based on the five-point clinical dementia rating (CDR) score.[48] Individuals with CDR scores of 0, 0.5, and greater than 0.5 were considered to have a diagnosis of NCI, MCI, and AD, respectively. Individuals without a clinical diagnosis were excluded from analysis.

Genotyping data. Individuals were genotyped via Affymetrix Precision Medicine Array following the manufacturer's protocol with DNA extracted from brain via the QIAGEN GenePure kit. We followed the same approach to quality control as was used for the discovery dataset genetic data, including filtering on the basis of data completeness, HWE, MAF, European ancestry, and relatedness. After quality control, we had 460,954 common SNVs to test and 149 subjects with both proteomic and genetic data. Demographic and disease information on these subjects is available in Table S1.

GWAS and eQTL summary statistics

For comparison, we downloaded summary statistics of four large GWASs (average N > 382,000): Alzheimer disease,[49] Parkinson disease,[50] schizophrenia,[51] and neuroticism.[52] We also downloaded the summary statistics for a large meta-analysis of brain eQTLs[22] (n = 1,433). The four GWAS results were from individuals of European descent and were used to identify disease-associated variants at a significance threshold of 5×10^{-8}. The brain eQTL meta-analysis combined ROS/MAP genetic and transcriptomic data with genetic and transcriptomic data from the CommonMind Consortium[53] and defined eQTLs at a FDR of 5%.

Genetic and protein annotation data

Each tested protein was annotated with the number of protein-protein interactions on the basis of the number of interactions reported in BioGrid data.[54] Furthermore, Bystro[37] was used to annotate each tested genetic variant with combined annotation dependent depletion (CADD) scores,[55] genomic contexts (i.e., exonic, intronic, UTRs, intergenic), and substitution types (i.e., non-synonymous versus synonymous). The annotations used for genomic context and substitution type were taken from the RefSeq database.[56] Since a variant may be tested against the abundance of more than one protein, we revised the genomic context annotations to be test specific. That is, for each SNP-protein pair tested, a SNP with genic genomic context (i.e., exonic, intronic, UTR) was re-annotated to intergenic if the SNP is not within the gene of the paired protein.

Statistical analyses

Estimation of additional confounders

To reduce confounding due to population structure, we added the first ten principal components of the discovery and replication dataset genotype data as model covariates in all relevant analyses. For both datasets, all ten principal components had significant Tracey-Widom statistics (p value < 0.05). Additionally, unknown confounders in the proteomic data were estimated via surrogate variable analysis and the SVA package in R.[57,58] For proteomic data for both datasets, ten surrogate variables were built and added as model covariations in all relevant analyses. Since the protein data was generated from bulk tissue, it is likely that some of these surrogate variables represent cell type proportions.

Identification of pQTLs

We identified genetic variants associated with protein abundance in the brain by using linear regression to model protein abundance as a function of genotype. We reduced our computational and testing burden by investigating only the proximal genetic effects of common single nucleotide variants (SNVs). We tested the proximal genetic control of each protein by using linear regression to model protein abundance as a function of genotype for every common SNV (MAF > 0.05) within a 100 kb window around the protein-coding gene. This window size was chosen because the majority of reported eQTLs are located within 100 kb of the regulated gene.[59–61] The location of each protein coding gene was defined by the knownGene table (GRCh37/hg19 assembly) from the University of California, Santa Cruz (UCSC) table browser.[62] For each SNV-protein pair, we regressed genotype against protein abundance, assuming additive genetic effects and including clinical diagnosis, the first ten genetic principal components, and ten surrogate variables as covariates. Analyses that restricted samples to those with NCI at death included only the first ten principal components as covariates. SNVs where genotype was significantly associated with protein abundance at a FDR of 5% were declared protein quantitative trait loci (pQTLs; FDR $<$ 0.05). For each protein with more than one pQTL, we identified the independent pQTL signals via stepwise linear regression.

Quantification of replication rates

Replication rates were estimated via the π_1 statistic from the qvalue package in R.[63] This statistic, which estimates the proportion of non-null hypotheses on the basis of the p value distribution, is more robust than a simple overlap of significant results.[64] For each replication analysis, we examined the distribution of replication study p values for sites found to be significant in the discovery

Table 1. Identification of pQTLs

	Number of pQTLs	Number of genes
Tested	501,414	7,376
Significant at FDR < 0.05 [*independent*]	35,601 [*8,451*]	2,474

Independent pQTLs were identified via stepwise regression.

study (FDR < 0.05). To reduce the influence of linkage disequilibrium, we analyzed only the lead discovery QTLs for each gene (i.e., sites with the strongest associations).

Enrichment analyses

We used Fisher's exact tests to assess the enrichment of brain pQTLs among (1) variants annotated to different genomic contexts (i.e., exonic, intronic, UTRs, intergenic) and substitution types (i.e., non-synonymous versus synonymous), (2) brain eQTLs, and (3) disease-associated variants. The tests for enrichment of pQTLs among variants in different genomic contexts and of different substitution types included only sites that were both annotated and tested in the pQTL analysis. Similarly, the test for enrichment of pQTLs among eQTLs included only sites that were tested in both the pQTL analysis and brain eQTL meta-analysis.[22] In contrast, the tests for enrichment of pQTLs among disease-associated variants included all sites tested in the pQTL analysis regardless of testing status in the investigated GWASs.

Mediation analyses

Mediation analyses were performed with the mediation package[65] in R and data from participants in the discovery dataset with both RNA-seq and TMT protein data. To increase the stability of statistical power across tests, we only considered proteins with more than 170 samples with both RNA-seq that TMT protein data. The analyses assessed mRNA abundance as a mediator of the genetic effects on protein abundance through the comparison of linear regression models. For each pQTL-protein pair, a model where genotype predicts protein abundance was compared to a model where both genotype and mRNA abundance predict protein abundance. All models additionally included clinical cognitive diagnosis, the first ten genetic principal components, and ten surrogate variables as covariates. A significant reduction in the effect of genotype on protein abundance with the addition mRNA abundance as a covariate is consistent with mediation. We compared the mediation results with the results of a large eQTL meta-analysis[22] to avoid spurious results due to a limited sample size. For this comparison, the eQTL meta-analysis was subset to the sites included in the pQTL analysis.

Gene Ontology analyses

Gene Ontology (GO) analyses were performed to gain a better understanding of the proteins that were found to be under genetic control and have mRNA-mediated or mRNA-independent abundance. We used GOrilla[66] to assess whether any biological processes significantly associate with the sets of genes with mRNA-mediated or mRNA-independent pQTLs. GOrilla uses a minimal hypergeometric score to quantify the enrichment of each GO term. Each set of genes was independently compared to the entire set of genes included in mediation testing.

Results

pQTL discovery

We identified proximal brain pQTLs for 2,474 genes (Table 1). These variants explained an average of 8.5% of the variation in abundance of each protein (Figure S4) and were enriched for SNVs with higher MAFs (Figure S5). All pQTL summary statistics, regardless of significance, are available for visualization and download on the pQTL web application (see "Web resources").

Genomic context of pQTLs

To better understand the genomic context of the identified pQTLs, we performed enrichment analyses to assess the overlap of pQTLs and genomic annotations. We found the identified pQTLs to be over-represented among SNVs in coding regions and SNVs with non-synonymous variation (Figure 1, Table S2). Additionally, we compared the distribution of pQTL effect sizes by genomic annotation and found pQTLs in coding regions (i.e., exons and UTRs) to have significantly larger median effect sizes than pQTLs in non-coding regions ($p < 0.005$ for all pairwise Nemenyi tests; Figure S6A). Furthermore, within exonic pQTLs, which have the largest median effect size overall, we found pQTLs with non-synonymous variation to have significantly larger median effect sizes than pQTLs with synonymous variation (Figure S6B). We see this pattern at pQTLs with a reference allele that increases protein abundance (Kruskal-Wallis $\chi^2 = 7.3$, $p = 0.006$) as well as at pQTLs with a reference allele that decreases protein abundance (Kruskal-Wallis $\chi^2 = 8.1$, $p = 0.004$). We performed separate analyses on exonic pQTLs with positive and negative effects to reduce possible confounding due to protein quantification bias. Because rare peptides may not be included in the proteomic database and are less likely to be accurately quantified, exonic coding-variation is more likely to associate with a decrease in protein abundance. We observed the reference allele to associate with decreased protein abundance for 61% of all exonic pQTLs and 68% of exonic pQTLs with non-synonymous variation. Together, these results suggest that genetic variation that changes a coded amino acid tends to have a large influence on protein abundance.

Influence of disease on pQTL identification

The proteomic data was generated from post-mortem samples of older adults, of which 31% had a clinical diagnosis of Alzheimer disease (AD) at death. To assess the influence of AD on the identification of pQTLs, we compared the results of the pQTL analysis for the discovery dataset (N = 330), which was adjusted for clinical diagnosis at death, to individuals from the discovery dataset with no cognitive impairment at death (N = 144). We found the estimated genetic effects on protein abundance to have a

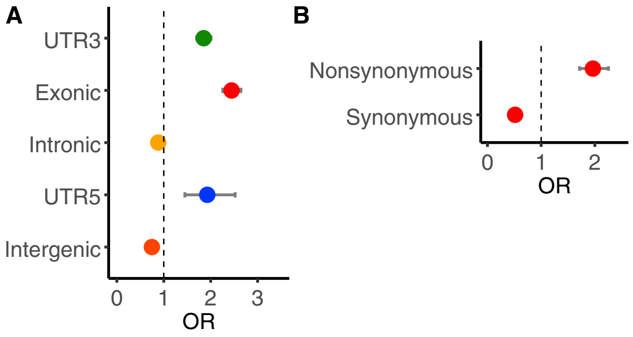

Figure 1. Enrichment of proximal pQTLs
(A) Enrichment of proximal pQTLs by genomic context.
(B) Enrichment of proximal pQTLs in exonic coding regions. For each annotation, enrichment was evaluated on the basis of a Fisher's exact tests assessing the overlap between pQTLs and the annotated SNVs. The estimated odds ratio (OR) and 95% confidence interval (CI) is shown for each test.

correlation of 0.62 between the main and control analyses (Figure S7; $p < 2.2 \times 10^{-16}$). Furthermore, we found this correlation to increase to 0.92 when we restricted to sites identified as pQTLs in the main analysis. This comparison suggests that AD has only a small influence on the identification of pQTLs in this study. The summary statistics from the control-only pQTL analysis are also available for visualization and download on the pQTL web application (see "Web resources").

Enrichment of brain disease-associated variants among pQTLs

Previous studies have shown that eQTLs tend to overlap with disease-associated variants identified by GWASs.[6–9] To assess whether variants associated with brain diseases are over-represented among the identified pQTLs, we performed a Fisher's exact test that compared the set of pQTLs to a set of SNVs that were identified to be disease associated by large GWASs of four brain disorders. We found the identified pQTLs to be highly enriched in brain disease-associated genetic variation (OR: 2.82, p value $= 1.6 \times 10^{-60}$; see Table S3 for individual disorder enrichments). The estimated enrichment supports the co-occurrence of pQTLs and disease-associated variants across the genome. However, further evaluation is needed to understand the functional consequences of these loci. Genetic colocalization methods, for example, could be used to mitigate false positives caused by linkage disequilibrium. The pQTL resource provided by this study will facilitate such analyses in the future.

pQTL replication

We assessed the replication rate of the identified brain pQTLs in an independent brain replication dataset,[47] which was comprised of genetic and proteomic data derived from the dPFC on 149 subjects of European descent. We identified proximal brain pQTLs for 1,803 genes in the replication dataset (Table S4). Next, we compared the 5,712 proteins that passed quality control and were analyzed in both the discovery and replication datasets. We used the π_1 statistic, which estimates the proportion of non-null hypotheses, to evaluate the replication rate of the brain pQTLs.[64] We found the pQTLs identified by the main analysis of data from the discovery dataset to be well replicated in the replication dataset ($\pi_1 = 0.77$). Furthermore, the estimated genetic effects on protein abundance in the discovery and replication analyses are highly correlated ($r = 0.90$, $p < 2.2 \times 10^{-16}$, Figure S8). These results indicate that the identified brain pQTLs are robust and not specific to an individual dataset.

Comparison of the genetic control of the human brain proteome and transcriptome

To quantify the extent to which genetic variation influences both mRNA and protein abundance in the brain, we examined the relationship between the pQTLs identified in this study and the eQTLs identified in a large meta-analysis of brain transciptomic data ($n = 1{,}433$).[22] Using simple overlap and enrichment methods, we found brain eQTLs to be significantly over-represented among brain pQTLs (OR: 7.42, 95% CI: [7.26,7.58], p value $< 2.2 \times 10^{-16}$), with the majority of brain pQTLs (61%) also identified as brain eQTLs. We also found that most of the sites identified to be both a pQTL and an eQTL have the same direction of effect on gene and protein expression (88%, Figure 2A). We additionally performed replication testing and found that the majority (75%) of genetic variants associated with protein abundance are also associated with mRNA abundance, but only the minority (40%) of genetic variants associated with mRNA abundance are also associated with protein abundance (Figure 2B). Furthermore, for variants that influence both mRNA and protein abundance, we found that the median effect size on protein abundance to be significantly lower than the median effect size on mRNA (Figure 2C; Kruskal-Wallis test $\chi^2 = 8{,}208$, $p < 2.2 \times 10^{-16}$). These observations, which have also been noted in lymphoblastoid cell lines,[15] are consistent with differences in mapping power between the pQTL and eQTLs studies as well as differences in evolutionary constraint on mRNA and protein.

Comparative studies across species have shown protein abundance to be less variable than mRNA.[67,68] These studies suggest that strong selective pressure maintains protein expression since large changes in protein abundances are likely to be deleterious given the pivotal roles of proteins in biological processes. To test whether there is evidence for evolutionary constraint on protein abundance, we examined the relationships between pQTL effects, MAFs, and CADD scores.[55] CADD scores are a quantitative measures of human variant deleteriousness that are highly related to evolutionary conservation. For pQTLs with large effects on protein abundance (in the top 10%), we observe a significant negative relationship between effect size and MAF (Figure S9, $p = 0.0006$) and a significant positive relationship between effect size and

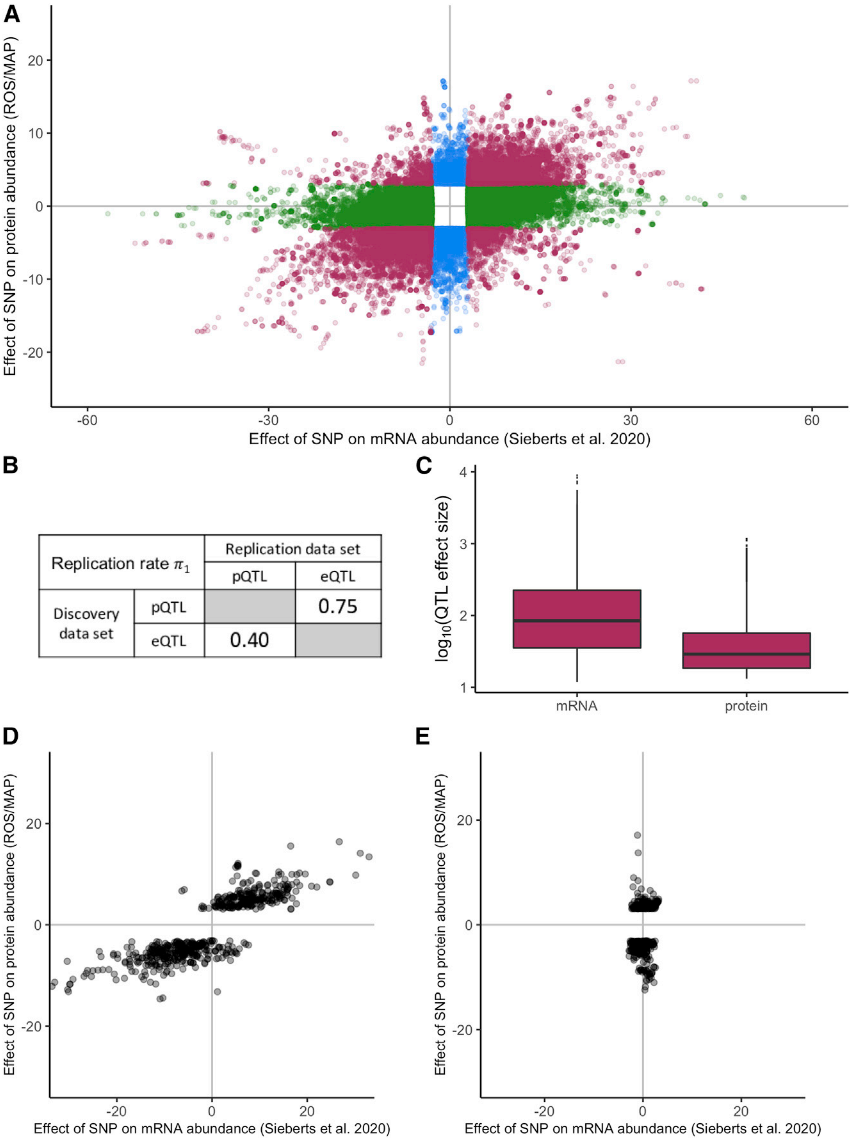

Replication rate π_1		Replication data set	
		pQTL	eQTL
Discovery data set	pQTL		0.75
	eQTL	0.40	

Figure 2. Comparisons between genetic effects on mRNA and protein abundance
(A) Comparison of the effect of each variant on mRNA and protein abundance. Each point represents one SNV tested against the abundance of the mRNA and protein of a single gene. The eQTLs (defined on the basis of False Discovery Rate [FDR] < 0.05) are shown in green, the pQTLs (defined on the basis of FDR < 0.05) are shown in blue, and the sites that are both an eQTL and a pQTL are shown in red. The shown effects are t-statistics.
(B) Replication rates (π_1) of pQTLs and eQTLs at FDR < 0.05. These analyses included the lead discovery QTLs for each gene tested in both studies.
(C) Comparison of the distribution of the size of genetic effects on mRNA and protein abundance for variants influencing both. The effect size is the absolute value of the pQTL or eQTL t-statistic. The boxes reflect the values corresponding to the first and third quartile, the horizontal line within the box reflects the median, the lines extending from the box represents the range of values within 1.5 times the interquartile range, and points beyond the line are plotted individually.
(D) Comparison of the genetic effects on mRNA and protein abundance for genes with protein expression mediated by mRNA.
(E) Comparison of the genetic effects on mRNA and protein abundance for genes with protein expression not mediated by mRNA. For all analyses the genetic effects on protein and mRNA abundance were from the discovery ROSMAP pQTL results and Sieberts et al. (2020),[22] respectively.

CADD score (Figure S10, $p = 0.018$). These results suggest that genetic variation that has a large impact on protein abundance tends to be rare and deleterious. Furthermore, we observe a significant negative relationship between the effect size of the lead pQTL for each gene and the number of protein-protein interactions for the corresponding protein (Figure S11, $p = 8.63 \times 10^{-8}$). This suggests that pQTLs for proteins with a larger number of interacting partners, which may indicate importance in cellular functioning, tend to have smaller effect sizes. Together, these observations support the notion that protein abundance is evolutionarily constrained.

Mediation of the genetic effects on protein by mRNA

To further investigate the influence of genetic variation on mRNA and protein abundance, we examined 173 individuals in the discovery dataset with genetic, transcriptomic, and proteomic data. The goal of this analysis was to identify whether there are distinct classes of proteins with underlying genetic variation that affects protein abundance through mRNA versus independent of mRNA. To infer this, we considered each independent pQTL and tested whether the genetic effect on protein was mediated by mRNA by using linear regression. To avoid spurious results due to a limited sample size, we considered a pQTL to be consistent with mRNA mediation only if the following were true: (1) mRNA abundance is a significant mediator of the genetic effect on protein abundance (FDR < 0.05) and (2) an eQTL has been identified for the corresponding gene in the large eQTL meta-analysis by Sieberts et al. (2020).[22] ($n = 1,433$; FDR < 0.05). Similarly, we considered a pQTL to not be consistent with mRNA mediation if the following are true: (1) mRNA abundance is not a significant mediator of the genetic effect on protein abundance (FDR > 0.05) and (2) an eQTL has not been identified for the corresponding gene in the large eQTL meta-analysis (FDR > 0.05). For ease, we call pQTLs meeting the first and second set of conditions mRNA-mediated and mRNA-independent pQTLs, respectively.

Using these criteria, we found 10.5% of pQTLs to be mRNA mediated ($n = 550/5,218$) and 6.5% of pQTLs to be mRNA independent ($n = 341/5,218$). For mRNA-mediated pQTLs, we found the genetic effect of each variant on protein and mRNA abundance to be significantly correlated (Figure 2D; $r = 0.85$; $p < 2.2 \times 10^{-16}$). Notably, the genetic effects of mRNA-mediated pQTLs tend to be smaller on protein abundance than mRNA, and the associated genes were not found to be enriched for any particular biological process (see Table S5 for a list of all investigated genes). As expected for mRNA-independent pQTLs, the genetic effect of each variant on protein and mRNA abundance was found to be uncorrelated (Figure 2E; $r = 0.1$, $p = 0.08$). Interestingly, GO analyses revealed genes with mRNA-independent pQTLs to be enriched among genes involved in transepithelial transport and neuron apoptotic processes (enrichment score = 10.9 and unadjusted $p = 7.6 \times 10^{-4}$ for both terms).

Discussion

We performed a large-scale investigation into the proximal genetic control of the human brain proteome by using deep brain proteomic profiling in two independent datasets. From this investigation, we generated a resource of pQTL summary statistics for the genetics and neuroscience communities that is accessible on the pQTL web application (see "Web resources"). The identified pQTLs in the discovery dataset tend to be non-synonymous variation, are over-represented among variants associated with brain diseases, and replicated well in an independent replication dataset.

We found that the majority of genetic variation that influences protein abundance also influences mRNA abundance but that the reverse is not true. That is, most pQTLs are eQTLs, but most eQTLs are not pQTLs. This result is potentially consistent with both reduced power to map pQTLs and greater evolutionary constraint on protein abundance. The latter is additionally supported by our observations of pQTLs with large effects' tending to be rare, deleterious, and associated with proteins that are less important to cellular functioning. These observations supplement previously reported evidence of purifying selection removing genetic variation that causes large deleterious changes to protein abundances.[15,67,68]

Mediation analyses using matched genetic, transcriptomic, and proteomic data provided evidence of mRNA-mediated and mRNA-independent genetic effects on protein abundance. We identified roughly 1.6 times more mRNA-mediated pQTLs than mRNA-independent pQTLs. This suggests that the genetic effects on protein abundances often, but not always, act through mRNA and the regulation of gene expression. We found genes with mRNA-independent pQTLs to be enriched in transepithelial transport and neuron apoptotic processes but genes with mRNA-mediated pQTLs to not be enriched in any particular biological process. The lack of enrichment in biological processes for genes with mRNA-mediated pQTLs may suggest that mRNA typically mediates protein abundance; however, we were only able to find evidence of mediation for a small subset of genes due to limited power. In contrast, the observation that genes with mRNA-independent pQTLs are significantly over-represented among genes involved in transepithelial transport and neuron apoptotic processes may indicate a de-coupling of mRNA and protein abundance in certain contexts of the older human brain. Similar independence between mRNA and protein abundance has been observed in nonreplicating mouse muscle cells.[69] On average, protein half-lives are reported to be at least five times longer than that of mRNA,[70] which could allow for de-coupling of mRNA and protein abundance. These results are consistent with the mediation of mRNA-independent pQTL effects through translational or post-translational regulation, such as protein degradation; however, this investigation is unable to implicate any specific gene regulation step or mechanism.

Human blood pQTL analyses have reported results similar to those presented here. These studies show an overlap between blood pQTLs and GWAS variants, as well as evidence that blood pQTLs are often, but not always, also eQTLs.[14,16,17] This suggests that although QTLs may be tissue specific or cell type specific, the relationships that we observe between disease and the genetic control of gene and protein expression are robust and generalizable.

A strength of our study was the ability to profile a total of 12,691 unique proteins from the human brain. This proteomic depth was achieved via TMT isobaric labeling coupled with high-pH offline fractionation following well-established protocols.[71] Those technical advantages enabled analysis of 7,376 proteins to be tested for a pQTL and identification of 2,474 proteins with a proximal pQTL. We tested the genetic variation within 100 kb of each protein coding gene and did not investigate more distal regulatory variants, which is a limitation of our analysis. The protein data missingness structure and sample size also potentially limits our ability draw inferences on low frequency SNVs and low abundant proteins. Another possible limitation of the proteomic data was the use of MS2 acquisition, which can suffer from the presence of co-isolated and co-fragmented interfering ions that can obscure quantification.[72] However, high-pH offline fractionation largely mitigates this issue.[71] Finally, the mediation analyses were most likely limited by power because of a small number of samples with matched brain-derived transcriptomic and proteomic data. Despite these limitations, our study provides a comprehensive assessment of proximal human brain pQTLs, a web-based resource for future investigations, and insight into the relationship between the genetic control of the human brain proteome and transcriptome.

Data and code availability

Phenotypic, proteomic, and genetic data used in this manuscript are available via the AD Knowledge Portal (https://adknowledgeportal.org). The AD Knowledge Portal is a platform for accessing data, analyses, and tools generated by the Accelerating Medicines Partnership (AMP-AD) Target Discovery Program and other National Institute on Aging (NIA)-supported programs to enable open-science practices and accelerate translational learning. The data, analyses, and tools are shared early in the research cycle without a publication embargo on secondary use. Data are available for general research use according to the following requirements for data access and data attribution (https://adknowledgeportal.synapse.org/DataAccess/Instructions). For this study, the data and results are available at https://doi.org/10.7303/syn24172458. The accession number for the data and results reported in this paper is Synapse: syn24172458.

Supplemental information

Supplemental information can be found online at https://doi.org/10.1016/j.ajhg.2021.01.012.

Acknowledgments

We thank the study participants, study partners, and staff of the ROS, MAP, and Brain and Body Donation Program studies. Support for this research was provided by the following grants from the US National Institutes of Health: T32 NS007480-18 (C.R.), R01 AG056533 (A.P.W. and T.S.W.), R01AG036042 (D.A.B. and P.L.D.), R01AG017917 (D.A.B.), R01AG015819 (D.A.B.), P30AG10161 (D.A.B.), and U01 AG46152 and U01AG061356 (P.L.D. and D.A.B.). Data collection was supported through funding by NIA grants P30AG10161, R01AG15819, R01AG17917, R01AG30146, R01AG36836, U01AG32984, U01AG46152, and U01AG61356; the Illinois Department of Public Health; and the Translational Genomics Research Institute. The Brain and Body Donation Program has been supported by U24 NS072026, P30 AG19610, the Arizona Department of Health Services, the Arizona Biomedical Research Commission, and the Michael J. Fox Foundation for Parkinson's Research. A.P.W. was also supported by a grant from the US Veterans Administration (BX003853) and US National Institute of Health U01 MH115484. T.S.W. was also supported by the US National Institute of Aging (P50 AG025688, R56 AG062256, R56 AG060757, U01 AG061357, U01 AG057195, and RF1 AG051633). The funders had no role in study design, data collection and analysis, decision to publish, or preparation of the manuscript. The views expressed in this work do not necessarily represent the views of the Veterans Administration or the United States Government.

Declaration of interests

C.R. is currently an employee of GlaxoSmithKline.

Received: October 2, 2020
Accepted: January 19, 2021
Published: February 10, 2021

Web resources

pQTL web application, https://brainqtl.org

References

1. Hormozdiari, F., Gazal, S., van de Geijn, B., Finucane, H.K., Ju, C.J., Loh, P.R., Schoech, A., Reshef, Y., Liu, X., O'Connor, L., et al. (2018). Leveraging molecular quantitative trait loci to understand the genetic architecture of diseases and complex traits. Nat. Genet. *50*, 1041–1047.
2. Pickrell, J.K., Marioni, J.C., Pai, A.A., Degner, J.F., Engelhardt, B.E., Nkadori, E., Veyrieras, J.B., Stephens, M., Gilad, Y., and Pritchard, J.K. (2010). Understanding mechanisms underlying human gene expression variation with RNA sequencing. Nature *464*, 768–772.
3. Lappalainen, T., Sammeth, M., Friedländer, M.R., 't Hoen, P.A., Monlong, J., Rivas, M.A., Gonzàlez-Porta, M., Kurbatova, N., Griebel, T., Ferreira, P.G., et al.; Geuvadis Consortium (2013). Transcriptome and genome sequencing uncovers functional variation in humans. Nature *501*, 506–511.
4. Zhu, Z., Zhang, F., Hu, H., Bakshi, A., Robinson, M.R., Powell, J.E., Montgomery, G.W., Goddard, M.E., Wray, N.R., Visscher, P.M., and Yang, J. (2016). Integration of summary data from GWAS and eQTL studies predicts complex trait gene targets. Nat. Genet. *48*, 481–487.
5. Battle, A., Brown, C.D., Engelhardt, B.E., Montgomery, S.B., et al.; GTEx Consortium; Laboratory, Data Analysis &Coordinating Center (LDACC)—Analysis Working Group; Statistical Methods groups—Analysis Working Group; Enhancing GTEx (eGTEx) groups; NIH Common Fund; and NIH/NCI (2017). Genetic effects on gene expression across human tissues. Nature *550*, 204–213.
6. Nicolae, D.L., Gamazon, E., Zhang, W., Duan, S., Dolan, M.E., and Cox, N.J. (2010). Trait-associated SNPs are more likely to be eQTLs: annotation to enhance discovery from GWAS. PLoS Genet. *6*, e1000888.
7. Hormozdiari, F., van de Bunt, M., Segrè, A.V., Li, X., Joo, J.W.J., Bilow, M., Sul, J.H., Sankararaman, S., Pasaniuc, B., and Eskin, E. (2016). Colocalization of GWAS and eQTL Signals Detects Target Genes. Am. J. Hum. Genet. *99*, 1245–1260.
8. Ongen, H., Brown, A.A., Delaneau, O., Panousis, N.I., Nica, A.C., Dermitzakis, E.T., Dermitzakis, E.T.; and GTEx Consortium (2017). Estimating the causal tissues for complex traits and diseases. Nat. Genet. *49*, 1676–1683.
9. Gamazon, E.R., Wheeler, H.E., Shah, K.P., Mozaffari, S.V., Aquino-Michaels, K., Carroll, R.J., Eyler, A.E., Denny, J.C., Nicolae, D.L., Cox, N.J., Im, H.K.; and GTEx Consortium (2015). A gene-based association method for mapping traits using reference transcriptome data. Nat. Genet. *47*, 1091–1098.
10. Wainberg, M., Sinnott-Armstrong, N., Mancuso, N., Barbeira, A.N., Knowles, D.A., Golan, D., Ermel, R., Ruusalepp, A., Quertermous, T., Hao, K., et al. (2019). Opportunities and challenges for transcriptome-wide association studies. Nat. Genet. *51*, 592–599.
11. Zhang, B., Wang, J., Wang, X., Zhu, J., Liu, Q., Shi, Z., Chambers, M.C., Zimmerman, L.J., Shaddox, K.F., Kim, S., et al.; NCI CPTAC (2014). Proteogenomic characterization of human colon and rectal cancer. Nature *513*, 382–387.
12. de Sousa Abreu, R., Penalva, L.O., Marcotte, E.M., and Vogel, C. (2009). Global signatures of protein and mRNA expression levels. Mol. Biosyst. *5*, 1512–1526.
13. Wu, L., Candille, S.I., Choi, Y., Xie, D., Jiang, L., Li-Pook-Than, J., Tang, H., and Snyder, M. (2013). Variation and genetic control of protein abundance in humans. Nature *499*, 79–82.

14. Emilsson, V., Ilkov, M., Lamb, J.R., Finkel, N., Gudmundsson, E.F., Pitts, R., Hoover, H., Gudmundsdottir, V., Horman, S.R., Aspelund, T., et al. (2018). Co-regulatory networks of human serum proteins link genetics to disease. Science *361*, 769–773.
15. Battle, A., Khan, Z., Wang, S.H., Mitrano, A., Ford, M.J., Pritchard, J.K., and Gilad, Y. (2015). Genomic variation. Impact of regulatory variation from RNA to protein. Science *347*, 664–667.
16. Sun, B.B., Maranville, J.C., Peters, J.E., Stacey, D., Staley, J.R., Blackshaw, J., Burgess, S., Jiang, T., Paige, E., Surendran, P., et al. (2018). Genomic atlas of the human plasma proteome. Nature *558*, 73–79.
17. Suhre, K., Arnold, M., Bhagwat, A.M., Cotton, R.J., Engelke, R., Raffler, J., Sarwath, H., Thareja, G., Wahl, A., DeLisle, R.K., et al. (2017). Connecting genetic risk to disease end points through the human blood plasma proteome. Nat. Commun. *8*, 14357.
18. Chick, J.M., Munger, S.C., Simecek, P., Huttlin, E.L., Choi, K., Gatti, D.M., Raghupathy, N., Svenson, K.L., Churchill, G.A., and Gygi, S.P. (2016). Defining the consequences of genetic variation on a proteome-wide scale. Nature *534*, 500–505.
19. Imming, P., Sinning, C., and Meyer, A. (2006). Drugs, their targets and the nature and number of drug targets. Nat. Rev. Drug Discov. *5*, 821–834.
20. Ng, B., White, C.C., Klein, H.U., Sieberts, S.K., McCabe, C., Patrick, E., Xu, J., Yu, L., Gaiteri, C., Bennett, D.A., et al. (2017). An xQTL map integrates the genetic architecture of the human brain's transcriptome and epigenome. Nat. Neurosci. *20*, 1418–1426.
21. Ramasamy, A., Trabzuni, D., Guelfi, S., Varghese, V., Smith, C., Walker, R., De, T., Coin, L., de Silva, R., Cookson, M.R., et al.; UK Brain Expression Consortium; and North American Brain Expression Consortium (2014). Genetic variability in the regulation of gene expression in ten regions of the human brain. Nat. Neurosci. *17*, 1418–1428.
22. Sieberts, S.K., Perumal, T.M., Carrasquillo, M.M., Allen, M., Reddy, J.S., Hoffman, G.E., Dang, K.K., Calley, J., Ebert, P.J., Eddy, J., et al.; CommonMind Consortium (CMC); and The AMP-AD Consortium (2020). Large eQTL meta-analysis reveals differing patterns between cerebral cortical and cerebellar brain regions. Sci. Data *7*, 340.
23. O'Brien, H.E., Hannon, E., Hill, M.J., Toste, C.C., Robertson, M.J., Morgan, J.E., McLaughlin, G., Lewis, C.M., Schalkwyk, L.C., Hall, L.S., et al. (2018). Expression quantitative trait loci in the developing human brain and their enrichment in neuropsychiatric disorders. Genome Biol. *19*, 194.
24. Kim, S., Cho, H., Lee, D., and Webster, M.J. (2012). Association between SNPs and gene expression in multiple regions of the human brain. Transl. Psychiatry *2*, e113.
25. Kim, Y., Xia, K., Tao, R., Giusti-Rodriguez, P., Vladimirov, V., van den Oord, E., and Sullivan, P.F. (2014). A meta-analysis of gene expression quantitative trait loci in brain. Transl. Psychiatry *4*, e459.
26. Gamazon, E.R., Badner, J.A., Cheng, L., Zhang, C., Zhang, D., Cox, N.J., Gershon, E.S., Kelsoe, J.R., Greenwood, T.A., Nievergelt, C.M., et al. (2013). Enrichment of cis-regulatory gene expression SNPs and methylation quantitative trait loci among bipolar disorder susceptibility variants. Mol. Psychiatry *18*, 340–346.
27. Sng, L.M.F., Thomson, P.C., and Trabzuni, D. (2019). Genome-wide human brain eQTLs: In-depth analysis and insights using the UKBEC dataset. Sci. Rep. *9*, 19201.
28. Bennett, D.A., Schneider, J.A., Buchman, A.S., Barnes, L.L., Boyle, P.A., and Wilson, R.S. (2012). Overview and findings from the rush Memory and Aging Project. Curr. Alzheimer Res. *9*, 646–663.
29. Bennett, D.A., Buchman, A.S., Boyle, P.A., Barnes, L.L., Wilson, R.S., and Schneider, J.A. (2018). Religious Orders Study and Rush Memory and Aging Project. J. Alzheimers Dis. *64* (s1), S161–S189.
30. Bennett, D.A., Schneider, J.A., Arvanitakis, Z., and Wilson, R.S. (2012). Overview and findings from the religious orders study. Curr. Alzheimer Res. *9*, 628–645.
31. Johnson, E.C.B., Dammer, E.B., Duong, D.M., Ping, L., Zhou, M., Yin, L., Higginbotham, L.A., Guajardo, A., White, B., Troncoso, J.C., et al. (2020). Large-scale proteomic analysis of Alzheimer's disease brain and cerebrospinal fluid reveals early changes in energy metabolism associated with microglia and astrocyte activation. Nat. Med. *26*, 769–780.
32. Wingo, A.P., Fan, W., Duong, D.M., Gerasimov, E.S., Dammer, E.B., Liu, Y., Harerimana, N.V., White, B., Thambisetty, M., Troncoso, J.C., et al. (2020). Shared proteomic effects of cerebral atherosclerosis and Alzheimer's disease on the human brain. Nat. Neurosci. *23*, 696–700.
33. De Jager, P.L., Ma, Y., McCabe, C., Xu, J., Vardarajan, B.N., Felsky, D., Klein, H.U., White, C.C., Peters, M.A., Lodgson, B., et al. (2018). A multi-omic atlas of the human frontal cortex for aging and Alzheimer's disease research. Sci. Data *5*, 180142.
34. Li, H., and Durbin, R. (2009). Fast and accurate short read alignment with Burrows-Wheeler transform. Bioinformatics *25*, 1754–1760.
35. DePristo, M.A., Banks, E., Poplin, R., Garimella, K.V., Maguire, J.R., Hartl, C., Philippakis, A.A., del Angel, G., Rivas, M.A., Hanna, M., et al. (2011). A framework for variation discovery and genotyping using next-generation DNA sequencing data. Nat. Genet. *43*, 491–498.
36. McKenna, A., Hanna, M., Banks, E., Sivachenko, A., Cibulskis, K., Kernytsky, A., Garimella, K., Altshuler, D., Gabriel, S., Daly, M., and DePristo, M.A. (2010). The Genome Analysis Toolkit: a MapReduce framework for analyzing next-generation DNA sequencing data. Genome Res. *20*, 1297–1303.
37. Kotlar, A.V., Trevino, C.E., Zwick, M.E., Cutler, D.J., and Wingo, T.S. (2018). Bystro: rapid online variant annotation and natural-language filtering at whole-genome scale. Genome Biol. *19*, 14.
38. Purcell, S., Neale, B., Todd-Brown, K., Thomas, L., Ferreira, M.A., Bender, D., Maller, J., Sklar, P., de Bakker, P.I., Daly, M.J., and Sham, P.C. (2007). PLINK: a tool set for whole-genome association and population-based linkage analyses. Am. J. Hum. Genet. *81*, 559–575.
39. Patterson, N., Price, A.L., and Reich, D. (2006). Population structure and eigenanalysis. PLoS Genet. *2*, e190.
40. Altshuler, D.M., Gibbs, R.A., Peltonen, L., Altshuler, D.M., Gibbs, R.A., Peltonen, L., Dermitzakis, E., Schaffner, S.F., Yu, F., Peltonen, L., et al.; International HapMap 3 Consortium (2010). Integrating common and rare genetic variation in diverse human populations. Nature *467*, 52–58.
41. Levin, J.Z., Yassour, M., Adiconis, X., Nusbaum, C., Thompson, D.A., Friedman, N., Gnirke, A., and Regev, A. (2010). Comprehensive comparative analysis of strand-specific RNA sequencing methods. Nat. Methods *7*, 709–715.
42. Adiconis, X., Borges-Rivera, D., Satija, R., DeLuca, D.S., Busby, M.A., Berlin, A.M., Sivachenko, A., Thompson, D.A., Wysoker,

A., Fennell, T., et al. (2013). Comparative analysis of RNA sequencing methods for degraded or low-input samples. Nat. Methods *10*, 623–629.

43. Dobin, A., Davis, C.A., Schlesinger, F., Drenkow, J., Zaleski, C., Jha, S., Batut, P., Chaisson, M., and Gingeras, T.R. (2013). STAR: ultrafast universal RNA-seq aligner. Bioinformatics *29*, 15–21.

44. Logsdon, B., Perumal, T.M., Swarup, V., Wang, M., Funk, C., Gaiteri, C., Allen, M., Wang, X., Dammer, E., Srivastava, G., et al. (2019). Meta-analysis of the human brain transcriptome identifies heterogeneity across human AD coexpression modules robust to sample collection and methodological approach. bioRxiv. https://doi.org/10.1101/510420.

45. Hansen, K.D., Irizarry, R.A., and Wu, Z. (2012). Removing technical variability in RNA-seq data using conditional quantile normalization. Biostatistics *13*, 204–216.

46. Law, C.W., Chen, Y., Shi, W., and Smyth, G.K. (2014). voom: Precision weights unlock linear model analysis tools for RNA-seq read counts. Genome Biol. *15*, R29.

47. Beach, T.G., Adler, C.H., Sue, L.I., Serrano, G., Shill, H.A., Walker, D.G., Lue, L., Roher, A.E., Dugger, B.N., Maarouf, C., et al. (2015). Arizona Study of Aging and Neurodegenerative Disorders and Brain and Body Donation Program. Neuropathology *35*, 354–389.

48. Morris, J.C. (1993). The Clinical Dementia Rating (CDR): current version and scoring rules. Neurology *43*, 2412–2414.

49. Jansen, I.E., Savage, J.E., Watanabe, K., Bryois, J., Williams, D.M., Steinberg, S., Sealock, J., Karlsson, I.K., Hägg, S., Athanasiu, L., et al. (2019). Genome-wide meta-analysis identifies new loci and functional pathways influencing Alzheimer's disease risk. Nat. Genet. *51*, 404–413.

50. Nalls, M.A., Blauwendraat, C., Vallerga, C.L., Heilbron, K., Bandres-Ciga, S., Chang, D., Tan, M., Kia, D.A., Noyce, A.J., Xue, A., et al.; 23andMe Research Team; System Genomics of Parkinson's Disease Consortium; and International Parkinson's Disease Genomics Consortium (2019). Identification of novel risk loci, causal insights, and heritable risk for Parkinson's disease: a meta-analysis of genome-wide association studies. Lancet Neurol. *18*, 1091–1102.

51. Lam, M., Chen, C.Y., Li, Z., Martin, A.R., Bryois, J., Ma, X., Gaspar, H., Ikeda, M., Benyamin, B., Brown, B.C., et al.; Schizophrenia Working Group of the Psychiatric Genomics Consortium; Indonesia Schizophrenia Consortium; and Genetic REsearch on schizophreniA neTwork-China and the Netherlands (GREAT-CN) (2019). Comparative genetic architectures of schizophrenia in East Asian and European populations. Nat. Genet. *51*, 1670–1678.

52. Nagel, M., Jansen, P.R., Stringer, S., Watanabe, K., de Leeuw, C.A., Bryois, J., Savage, J.E., Hammerschlag, A.R., Skene, N.G., Muñoz-Manchado, A.B., et al.; 23andMe Research Team (2018). Meta-analysis of genome-wide association studies for neuroticism in 449,484 individuals identifies novel genetic loci and pathways. Nat. Genet. *50*, 920–927.

53. Fromer, M., Roussos, P., Sieberts, S.K., Johnson, J.S., Kavanagh, D.H., Perumal, T.M., Ruderfer, D.M., Oh, E.C., Topol, A., Shah, H.R., et al. (2016). Gene expression elucidates functional impact of polygenic risk for schizophrenia. Nat. Neurosci. *19*, 1442–1453.

54. Stark, C., Breitkreutz, B.J., Reguly, T., Boucher, L., Breitkreutz, A., and Tyers, M. (2006). BioGRID: a general repository for interaction datasets. Nucleic Acids Res. *34*, D535–D539.

55. Rentzsch, P., Witten, D., Cooper, G.M., Shendure, J., and Kircher, M. (2019). CADD: predicting the deleteriousness of variants throughout the human genome. Nucleic Acids Res. *47* (D1), D886–D894.

56. O'Leary, N.A., Wright, M.W., Brister, J.R., Ciufo, S., Haddad, D., McVeigh, R., Rajput, B., Robbertse, B., Smith-White, B., Ako-Adjei, D., et al. (2016). Reference sequence (RefSeq) database at NCBI: current status, taxonomic expansion, and functional annotation. Nucleic Acids Res. *44* (D1), D733–D745.

57. Leek, J.T., Johnson, W.E., Parker, H.S., Jaffe, A.E., and Storey, J.D. (2012). The sva package for removing batch effects and other unwanted variation in high-throughput experiments. Bioinformatics *28*, 882–883.

58. Leek, J.T., and Storey, J.D. (2007). Capturing heterogeneity in gene expression studies by surrogate variable analysis. PLoS Genet. *3*, 1724–1735.

59. Dixon, A.L., Liang, L., Moffatt, M.F., Chen, W., Heath, S., Wong, K.C., Taylor, J., Burnett, E., Gut, I., Farrall, M., et al. (2007). A genome-wide association study of global gene expression. Nat. Genet. *39*, 1202–1207.

60. Stranger, B.E., Nica, A.C., Forrest, M.S., Dimas, A., Bird, C.P., Beazley, C., Ingle, C.E., Dunning, M., Flicek, P., Koller, D., et al. (2007). Population genomics of human gene expression. Nat. Genet. *39*, 1217–1224.

61. Gilad, Y., Rifkin, S.A., and Pritchard, J.K. (2008). Revealing the architecture of gene regulation: the promise of eQTL studies. Trends Genet. *24*, 408–415.

62. Karolchik, D., Hinrichs, A.S., Furey, T.S., Roskin, K.M., Sugnet, C.W., Haussler, D., and Kent, W.J. (2004). The UCSC Table Browser data retrieval tool. Nucleic Acids Res. *32*, D493–D496.

63. Storey, J.D., Bass, A.J., Dabney, A., Robinson, D., and Warnes, G. (2020). qvalue: Q-value estimation for false discovery rate control (LGPL).

64. Storey, J.D., and Tibshirani, R. (2003). Statistical significance for genomewide studies. Proc. Natl. Acad. Sci. USA *100*, 9440–9445.

65. Tingley, D., Yamamoto, T., Hirose, K., Keele, L., and Imai, K. (2014). mediation: R Package for Causal Mediation Analysis. J. Stat. Softw. *59*, 1–38.

66. Eden, E., Navon, R., Steinfeld, I., Lipson, D., and Yakhini, Z. (2009). GOrilla: a tool for discovery and visualization of enriched GO terms in ranked gene lists. BMC Bioinformatics *10*, 48.

67. Laurent, J.M., Vogel, C., Kwon, T., Craig, S.A., Boutz, D.R., Huse, H.K., Nozue, K., Walia, H., Whiteley, M., Ronald, P.C., and Marcotte, E.M. (2010). Protein abundances are more conserved than mRNA abundances across diverse taxa. Proteomics *10*, 4209–4212.

68. Khan, Z., Ford, M.J., Cusanovich, D.A., Mitrano, A., Pritchard, J.K., and Gilad, Y. (2013). Primate transcript and protein expression levels evolve under compensatory selection pressures. Science *342*, 1100–1104.

69. Gross, M.K., and Merrill, G.F. (1988). Regulation of thymidine kinase protein levels during myogenic withdrawal from the cell cycle is independent of mRNA regulation. Nucleic Acids Res. *16*, 11625–11643.

70. Schwanhäusser, B., Busse, D., Li, N., Dittmar, G., Schuchhardt, J., Wolf, J., Chen, W., and Selbach, M. (2011). Global quantification of mammalian gene expression control. Nature *473*, 337–342.

71. Mertins, P., Tang, L.C., Krug, K., Clark, D.J., Gritsenko, M.A., Chen, L., Clauser, K.R., Clauss, T.R., Shah, P., Gillette, M.A., et al. (2018). Reproducible workflow for multiplexed deep-scale proteome and phosphoproteome analysis of tumor tissues by liquid chromatography-mass spectrometry. Nat. Protoc. *13*, 1632–1661.

72. McAlister, G.C., Nusinow, D.P., Jedrychowski, M.P., Wühr, M., Huttlin, E.L., Erickson, B.K., Rad, R., Haas, W., and Gygi, S.P. (2014). MultiNotch MS3 enables accurate, sensitive, and multiplexed detection of differential expression across cancer cell line proteomes. Anal. Chem. *86*, 7150–7158.

The American Journal of Human Genetics, Volume *108*

Supplemental data

Genetic control of the human brain proteome

Chloe Robins, Yue Liu, Wen Fan, Duc M. Duong, Jacob Meigs, Nadia V. Harerimana, Ekaterina S. Gerasimov, Eric B. Dammer, David J. Cutler, Thomas G. Beach, Eric M. Reiman, Philip L. De Jager, David A. Bennett, James J. Lah, Aliza P. Wingo, Allan I. Levey, Nicholas T. Seyfried, and Thomas S. Wingo

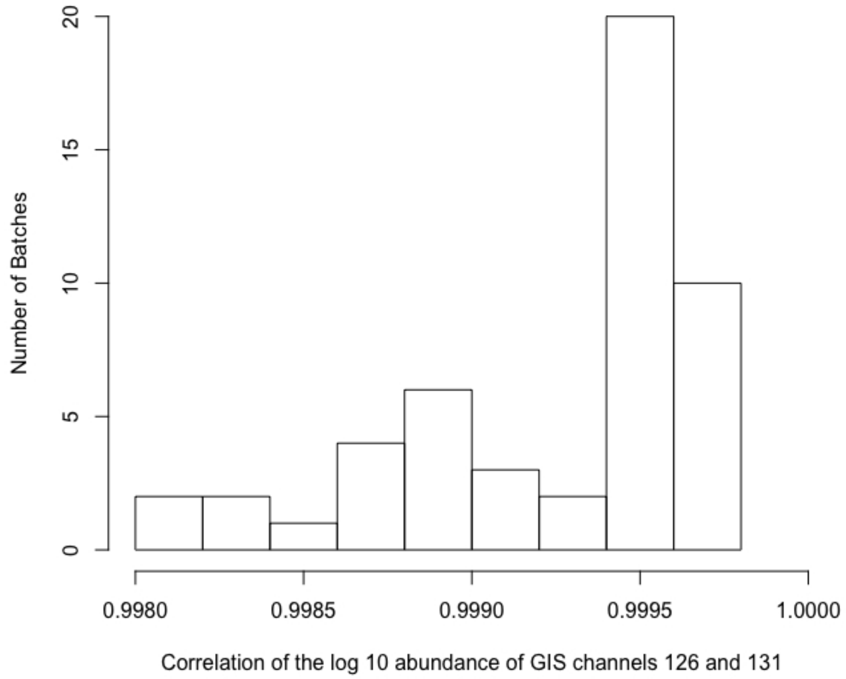

Figure S1. Distribution of the batch-specific correlation of GIS channels. Each TMT proteomic experiment, or batch, contains two GIS channels (126 and 131). Here we show the distribution of correlations of proteomic measurements between the batch-specific GIS channels.

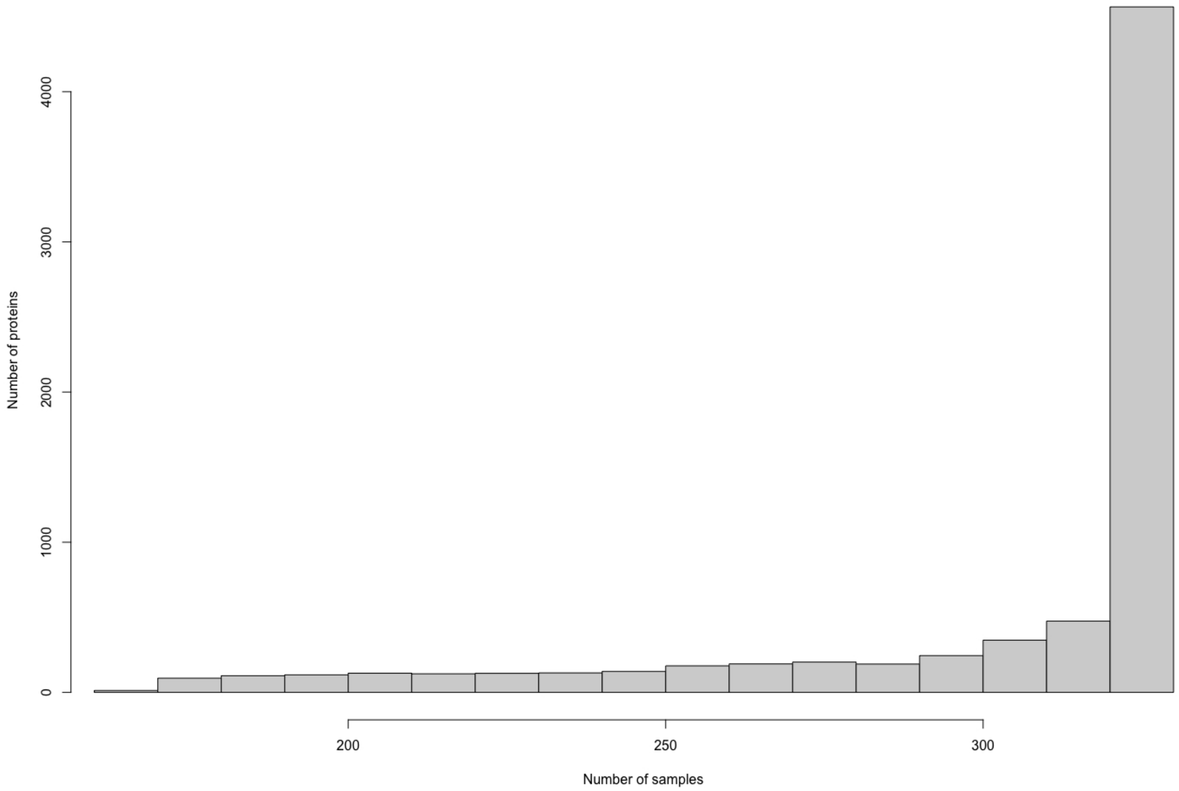

Figure S2. Distribution of the sample sizes used in the pQTL analyses. Due to the highly batch-specific nature of protein measurement in TMT proteomic experiments, each measured protein has a different sample size. This histogram shows the distribution of sample sizes across tested proteins.

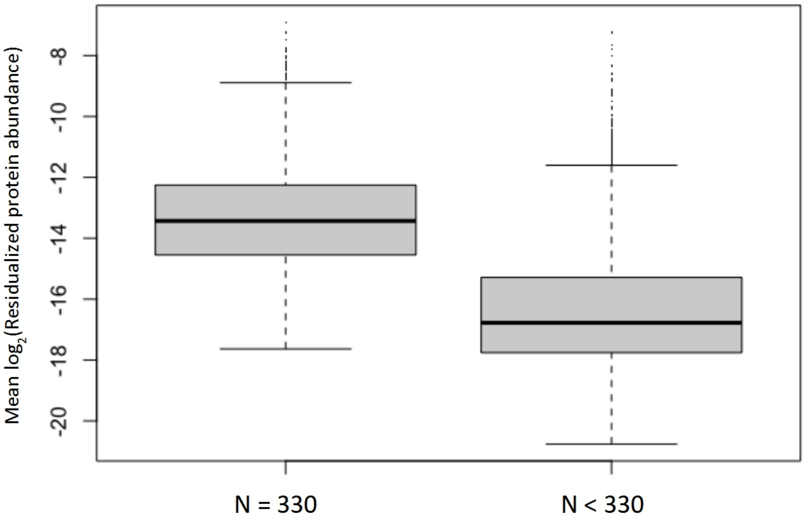

Figure S3. Comparison of the distribution of average protein abundances for proteins measured in all 330 participants (N = 3,843 proteins) vs. those with missing data (N = 4,173 proteins). The difference in distribution is significant by Kruskal-Wallis test (χ^2= 3378.7, p < 2.2x10^{-16}).

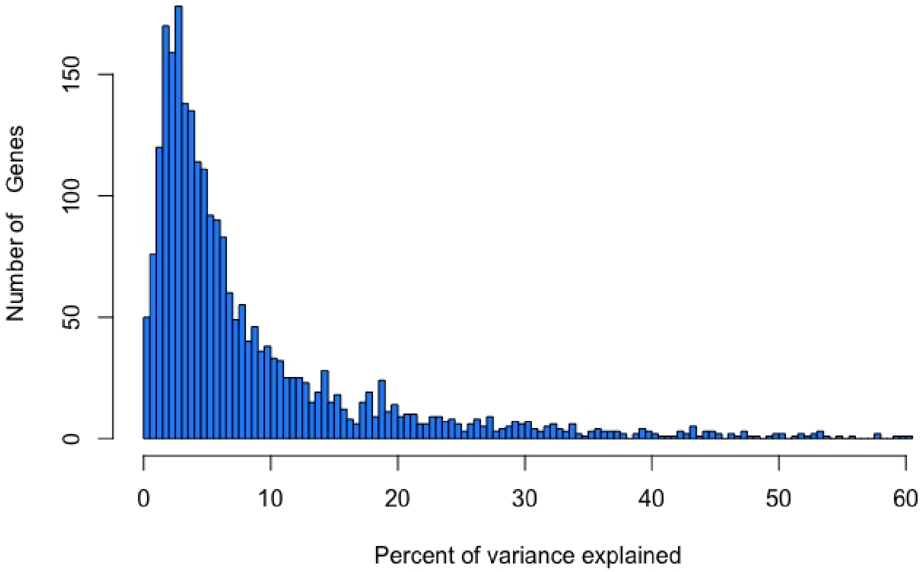

Figure S4. Percentage of variance in protein abundance explained by genotype. For the 2,474 genes with a genetic variant that significantly predicts protein abundance, we used stepwise linear regression to identify all independent pQTLs and assess the proportion of variance in protein abundance explained. The median and mean percentage of variance in protein abundance explained by pQTLs is 4.9% and 8.5% respectively.

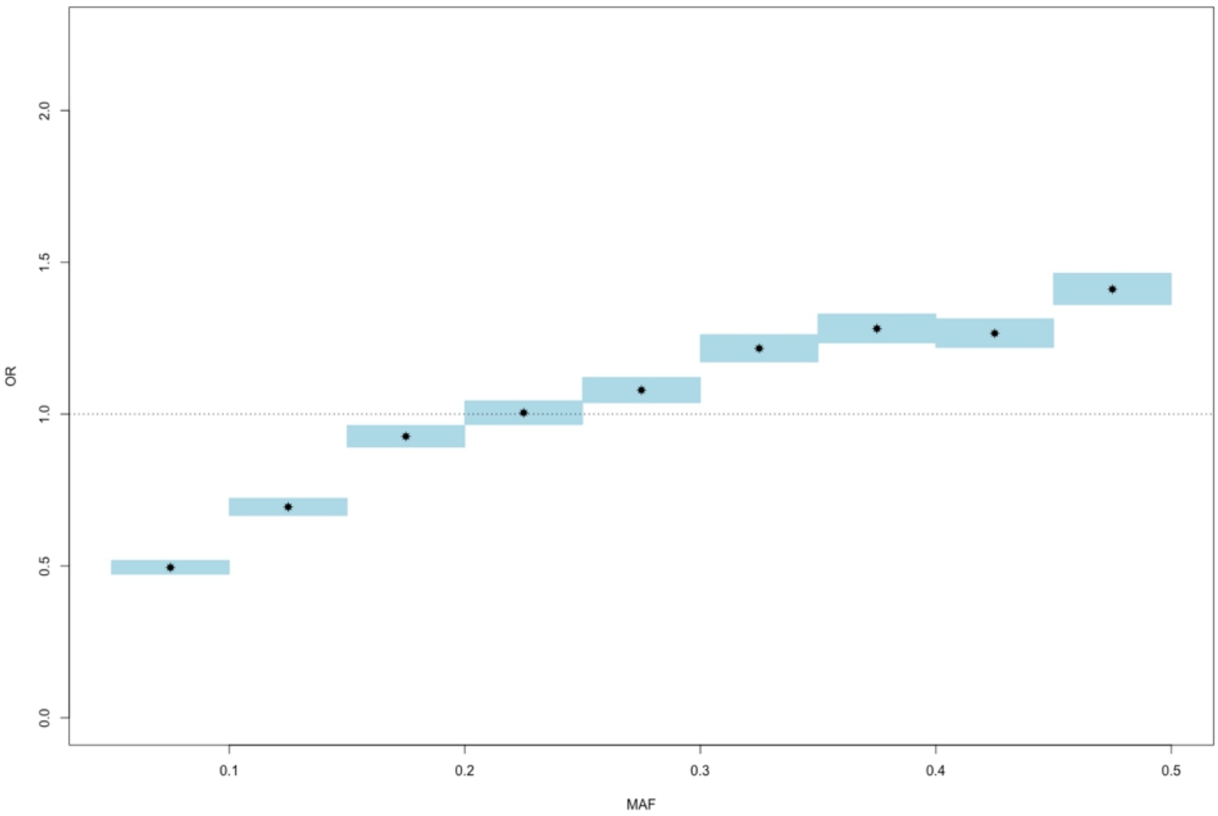

Figure S5. Enrichment of pQTL identification by MAF. Each blue rectangle represents the results of a Fisher's exact test. Each test compared the set of SNVs with a MAF within the range delineated by the blue rectangle and the set of SNVs identified as a pQTL. The height of the dot in the center of each rectangle shows the odds ratio estimate, while the estimate's 95% confidence interval is shown as the height of the rectangle. Tests with blue rectangles below the horizontal dashed line show significant depletion of pQTLs in SNVs with MAFs within the denoted range. Tests with blue rectangles above the horizontal dashed line show significant enrichment of pQTLs in SNVs with MAFs within the denoted range. Only proteins with complete data were considered for this analysis.

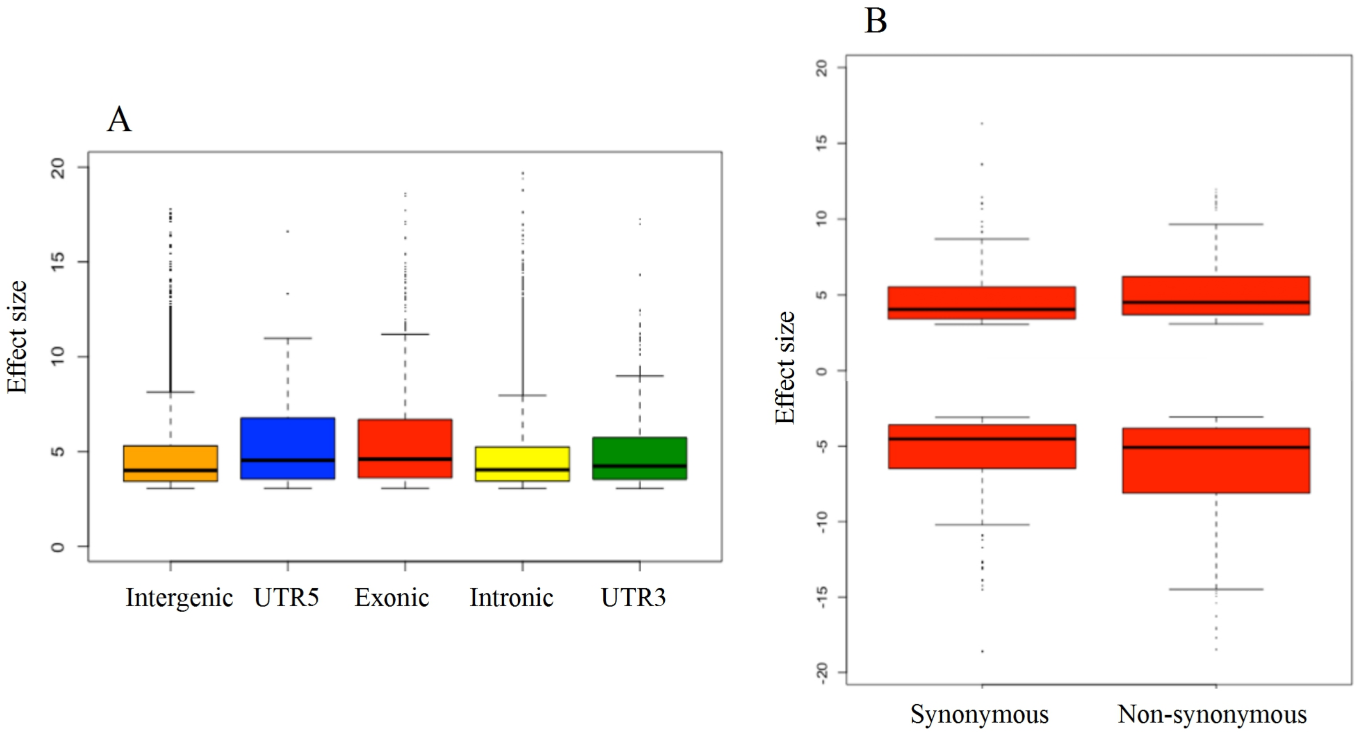

Figure S6. Effect size of pQTLs by genomic annotation. (A) Boxplots showing the distribution of pQTL effect sized by genic location. The shown effect size is the absolute value of the pQTL t-statistic. (B) Boxplots showing the distribution of positive and negative exonic pQTL effects for synonymous and non-synonymous variation.

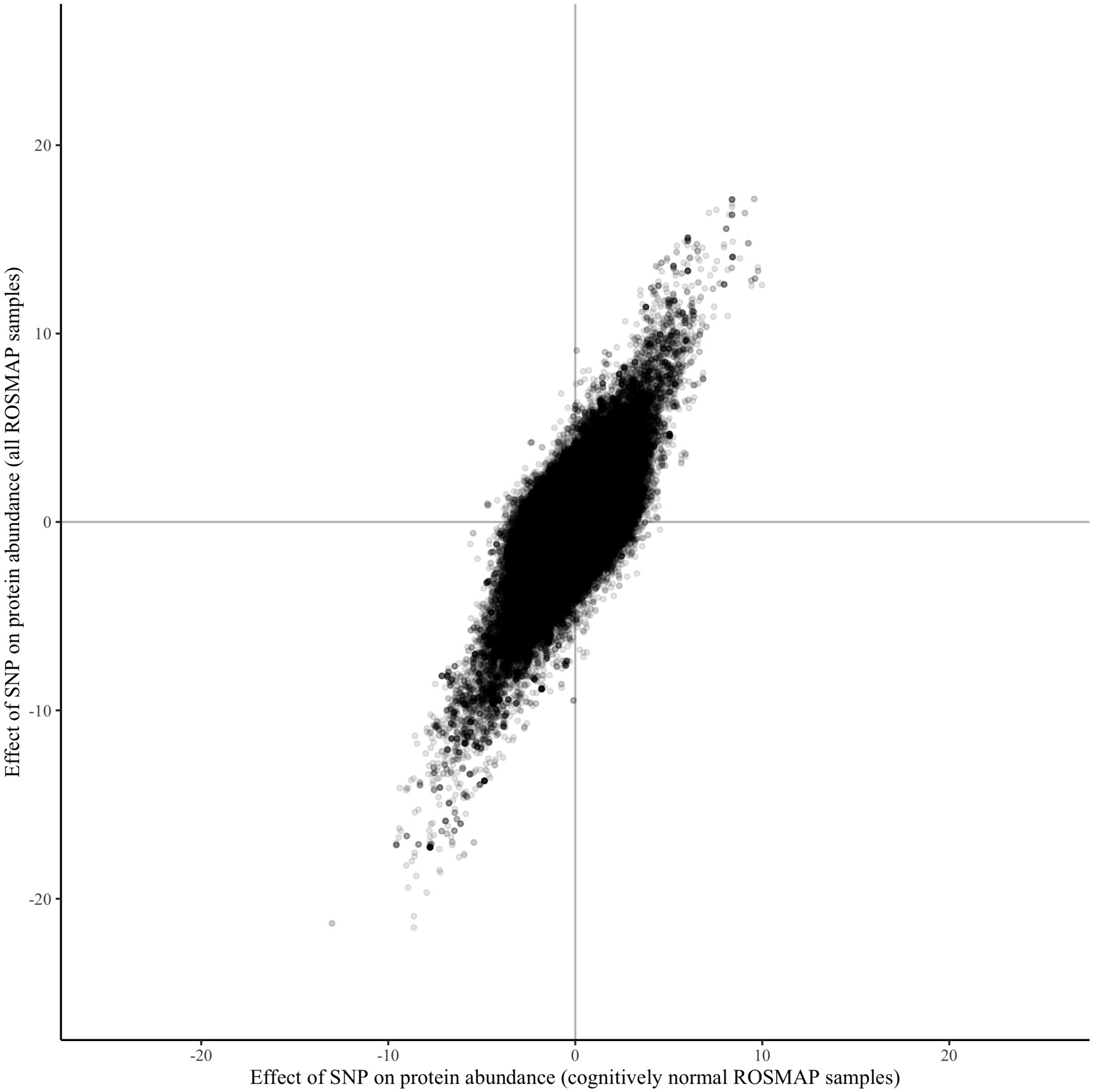

Figure S7. Comparison of pQTL effects estimated using samples with no cognitive impairment vs. all samples. Each point represents a test of a SNV against the protein expression of a single gene. The y-axis shows the effect of a SNV on protein abundance estimated by the main pQTL analysis that used 330 samples and adjusted for clinical diagnosis at death. The x-axis shows the effect of a SNV on protein abundance estimated by a pQTL analysis that used a subset of 139 samples with a clinical diagnosis of no cognitive impairment (NCI) at death. The shown effects are t-statistics. A total of 776,507 tests were performed in both analyses and were plotted here. The correlation between all estimated effects is 0.62 ($p<2.2x10^{-16}$), while the correlation between the estimated effects at sites identified as pQTLs in the main analysis is 0.92 ($p<2.2x10^{-16}$, 37,569 tests at FDR < 0.05).

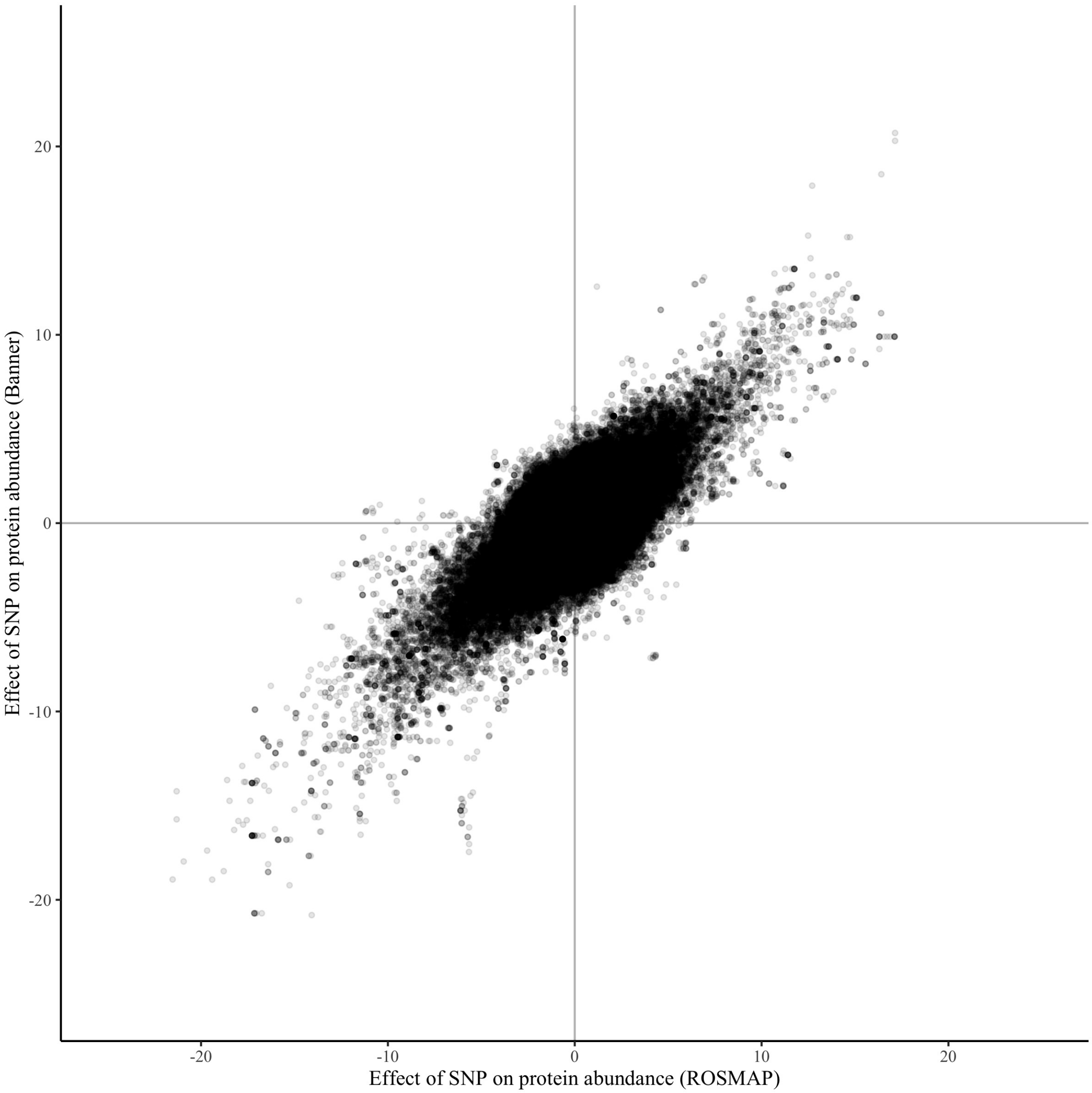

Figure S8. **Comparison of pQTL effects estimated using Banner vs. ROS/MAP samples.** Each point represents a test of a SNV against the protein expression of a single gene. The y-axis shows the effect of a SNV on protein abundance estimated by the Banner pQTL analysis, while the x-axis shows the effect of a SNV on protein abundance estimated by the ROS/MAP pQTL analysis. The shown effects are t-statistics. A total of 591,720 tests were performed in both analyses and were plotted here. The correlation between all estimated effects is 0.57 ($p<2.2x10^{-16}$), while the correlation between the estimated effects at sites identified as pQTLs in the ROS/MAP analysis is 0.90 ($p<2.2x10^{-16}$, 32,679 tests at FDR < 0.05).

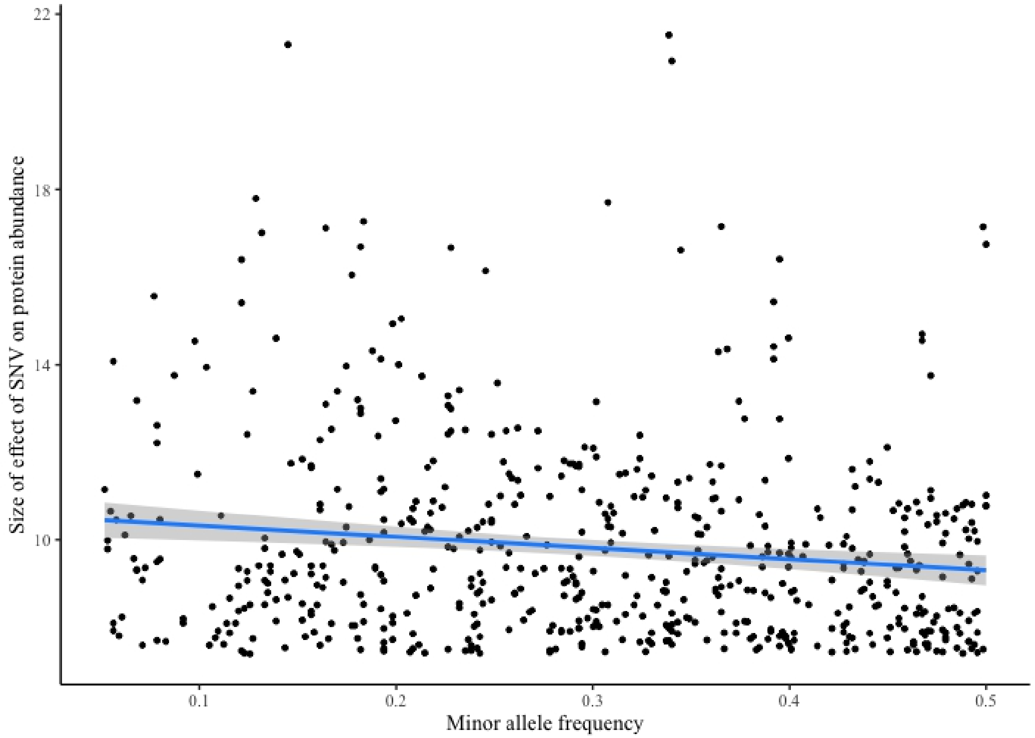

Figure S9. Relationship between pQTL effect size and minor allele frequency (MAF). For this analysis, we considered only independent pQTLs with effects sizes (absolute value of pQTL t-statistic) in the top 10%. The relationship between effect size and MAF was estimated based on a linear regression that modeled the absolute value of the pQTL t-statistic as a function of MAF. We found an increase in MAF to be associated with a decrease in the size of the genetic effect on protein (β =- 2.5479, p = 0.000634).

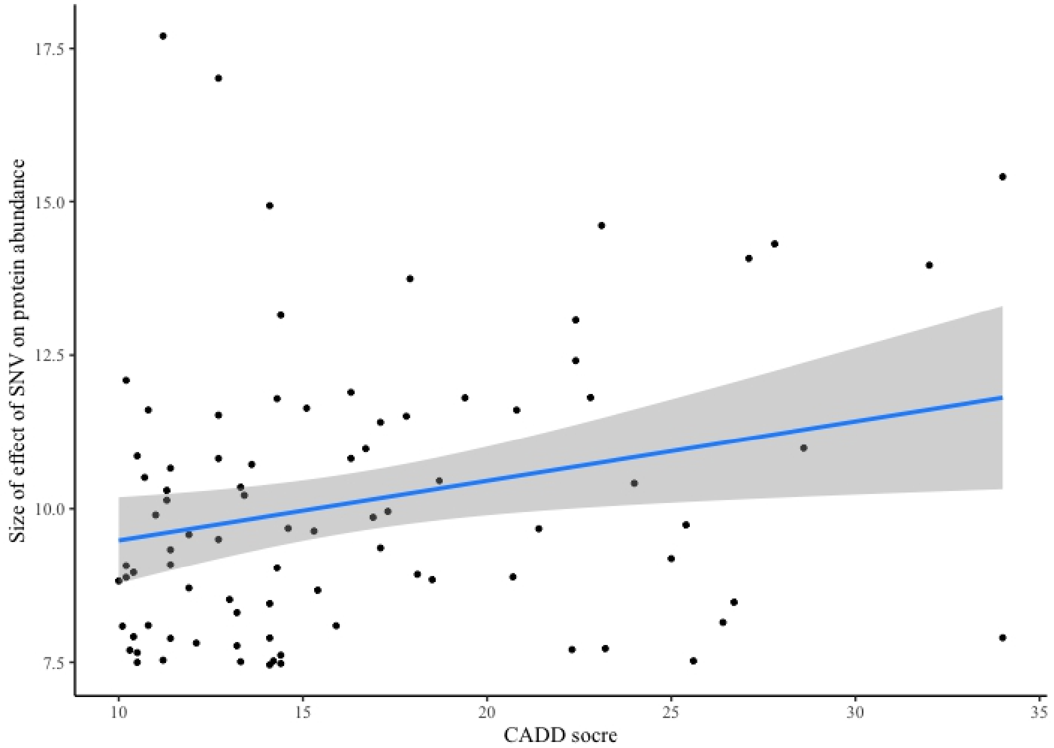

Figure S10. Relationship between pQTL effect size and CADD score. For this analysis, we considered only independent pQTLs with effect sizes (absolute value of pQTL t-statistic) in the top 10% and a CADD score greater than 10. Variants with a CADD score above 10 are predicted to be in the top 10% of deleterious variants in the human genome. The relationship between effect size and CADD score was estimated based on a linear regression that modeled the absolute value of the pQTL t-statistic as a function of CADD score. We found an increase in CADD score to be associated with an increase in the size of the genetic effect on protein (β= 0.09692 , p = 0.0186).

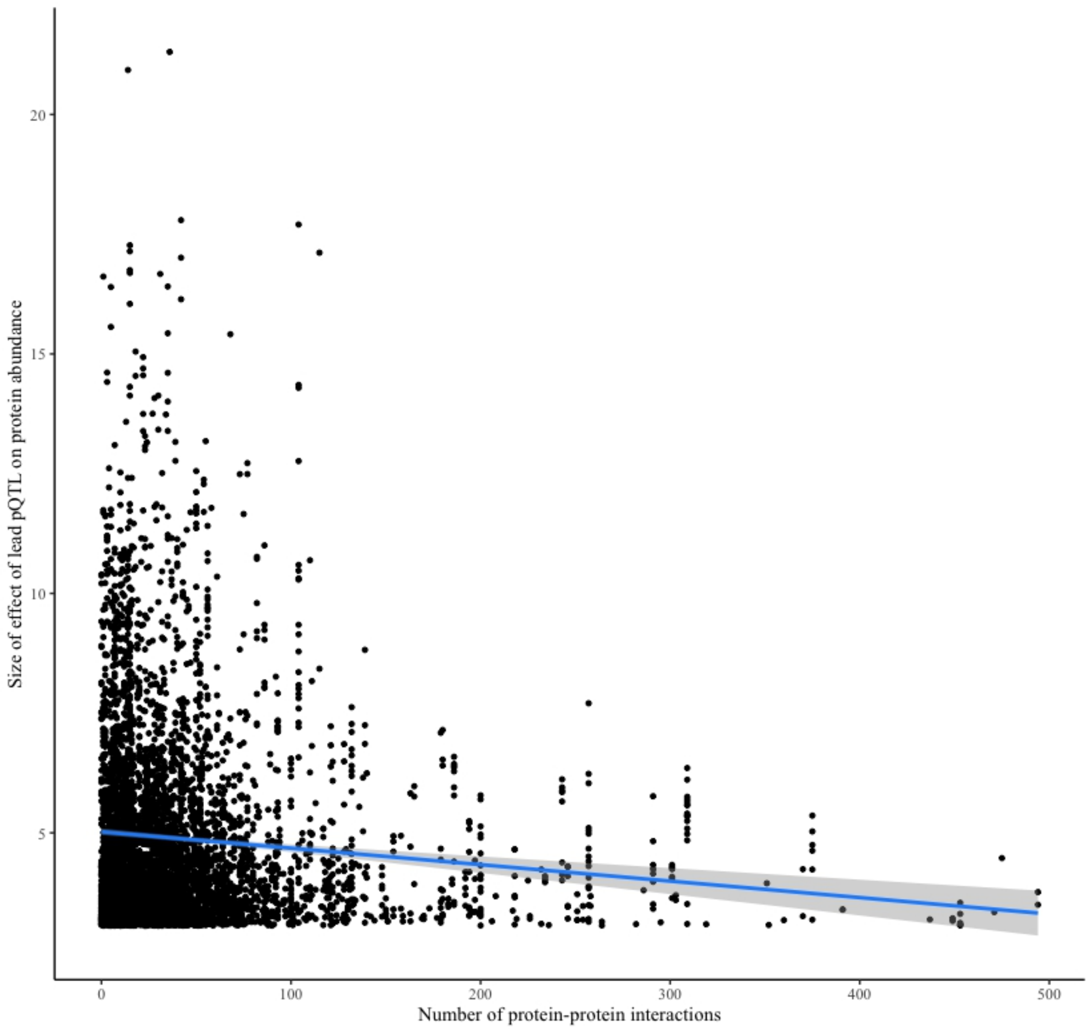

Figure S11. Relationship between the effect size of the lead pQTL and the number of protein-protein interactions. This analysis considered lead pQTLs for proteins with less than 500 protein-protein interactions. The relationship between effect size and number of protein-protein interactions was estimated based on a linear regression that modeled the absolute value of the pQTL t-statistic as a function of the number of protein-protein interactions. We found an increase in the number of protein-protein interactions to be associated with a decrease in the size of the genetic effect on protein (β = -0.001365, p = 1.09e-05).

Table S1. Demographics of analyzed subjects.

	ROS/MAP		Banner BBDP
Characteristic	**Subjects with protein and genotype data**	**Subjects with mRNA, protein, and genotype data**	**Subjects with protein and genotype data**
Sample Size	330	173	149
Female sex (%)	69%	69%	56%
Age at death [years] (median, range)	89 [71 – 106.5]	89 [71 – 106.5]	86 [66 – 103]
Clinical diagnosis of dementia (N, %)			
No cognitive impairment	139 (42%)	78 (45%)	64 (43%)
Mild cognitive impairment	90 (27%)	53 (31%)	20 (13%)
Alzheimer’s disease	101 (31%)	42 (24%)	65 (44%)

Table S2. Enrichment of genomic annotations among pQTLs. Enrichments were evaluated with Fisher's exact tests. With the exception of the synonymous and non-synonymous annotations, the background for every test was the set of all SNVs tested in our pQTL study. The background for the synonymous and non-synonymous annotations was the set of all tested exonic SNVs.

Annotation	**# SNVs**	**pQTL enrichment**		
		OR	**95% CI** Lower limit, upper limit	**P**
UTR3	6,654	1.85	1.70, 2.01	1.8e-42
Exonic	5,930	2.44	2.26, 2.64	5.3e-91
synonymous	*3,725*	*0.51*	*0.45, 0.59*	*5.27e-22*
non-synonymous	*2,172*	*1.96*	*1.71, 2.25*	*1.08e-22*
Intronic	218,202	0.88	0.86, 0.91	5.3e-20
UTR5	580	1.93	1.45, 2.52	8.4e-6
Intergenic	177,421	0.75	0.73, 0.77	6.1e-130

Table S3. Large GWASs of brain diseases used to assess the enrichment of disease variants among pQTLs. Only GWAS result from individuals of European descent were analyzed. For each GWAS we used a significance threshold of $5x10^{-8}$ to identify disease-associated variants within 100 kb of genes with proteomic data. Enrichment was assessed for each disease individually using Fischer exact tests.

Brain disease	**Study**	**N**	**# of disease-associated variants**	**# of overlapping pQTLs**	**Enrichment**	
					OR	**p-value**
Alzheimer's disease	Jansen *et al*. 2017	455,258	219	16	1.01	0.90
Parkinson's disease	Nalls *et al*. 2019	471,013	218	83	5.82	4.04e-31
Schizophrenia	Lam *et al*. 2019	154,192	778	142	2.61	4.86e-21
Neuroticism	Nagel *et al*. 2018	449,484	894	182	3.07	9.35e-34

Table S4. Comparison of pQTL identification using the ROS/MAP and Banner BBDP cohorts.

Cohort	Sample size	Number of tested SNVs	Number of tested genes	Number of pQTLs	Number of pQTL genes
ROSMAP	163-330	501,414	7,376	35,601	2,474
Banner BBDP	75-149	460,954	6,526	23,945	1,803
Overlap		429,083	5,712	14,752	1,129

Table S5. List of genes with mRNA-mediated and mRNA-independent pQTLs. Genes in bold are associated with the GO term "neuron apoptotic process". Genes in italic are associated with the GO term "transepithelial transport"

Chr	Genes with mRNA-mediated pQTLs	Genes with mRNA-independent pQTLs
1	RPA2, PADI2, AGL, CCBL2, KYAT3, DBT, SLC25A24, GSTM5, GSTM3, PTGFRN, S100A13, TDRKH, S100A4, TSTD1, DARS2, COA6, NTPCR	ARID1A, ENO1, NASP, ACOT7, SH3GLB1, USP24, BOLA1, CA14, LYSMD1, PSMB4, FDPS, CDC73, CACNA1E, GLUL, TROVE2, CNTN2, IARS2, CAPN2, CCSAP, NID1
2	DPYSL5, RETSAT, GALM, CAPG, PLCL1, ATIC, PPIL3, IDH1, SCRN3	BRE; BABAM2, HS1BP3, MRPL53, TGOLN2, INPP4A, LONRF2, CNTNAP5, TMEFF2, ABCB6, DOCK10
3	PLSCR4, ATG7, MYLK, LARS2, CHL1, LZTFL1	APPL1, CPOX, TF, CDV3, ADCY5, IQSEC1, TFRC
4	DGKQ, TBC1D1, PGM2, GUF1, GPRIN3, SPARCL1, HSD17B11, SCRG1, MMAA	PAICS, KIT
5	SGTB, ERAP1, DIAPH1, TBC1D9B, RUFY1	SLC1A3, SLC12A2, PPIP5K2, HINT1
6	ECI2, HDDC2, SIRT5, GOPC, RWDD1, CAP2, AKAP12, ACAT2, BPHL	ME1, RIMS1, RAB23
7	AMPH, EGFR, ABHD11, PDIA4, ABCB8	GARS, PMPCB, AGFG2, CCDC132; VPS50, SLC25A13, SSBP1, MKRN1
8	LY6H, ADHFE1, SNTB1	OXR1, RALYL, TATDN1, KHDRBS3, ATP6V1B2, GPT
9	AK3, ACO1, NUDT2, GLIPR2, PHYHD1, PTGR1, AIF1L, CCBL1; KYAT1, HDHD3	PSIP1, GBA2
10	SNCG, ANXA11, COX15, PRTFDC1, SFXN3, PRKG1	SEC24C, FAM175B; ABRAXAS2
11	AMPD3, SLC17A6, LRP4, HSD17B12, AAMDC, ASRGL1, C11orf54, MADD, SNX32	CEND1, TPP1, NUCB2, SPON1, SLC1A2, CAPRIN1, CTNND1, INPPL1, CFL1, ZBTB16, SIK3, MCAM, C2CD2L, DCPS
12	CPM, CORO1C, UHRF1BP1L, ESYT1, NT5DC3, ARHGDIB, PIP4K2C, CSRP2, MGST1	ISCU, CS, ANO6, RPAP3, NUAK1, CIT, CALCOCO1
13	CAB39L	DOCK9
14	L3HYPDH, PTGR2, DAAM1, ACOT1, STXBP6, STON2, INF2, ACOT2	HNRNPC, GPHN, COQ6, RTN1, ACYP1, VIPAS39, CDC42BPB
15	FAM82A2; RMDN3, RLBP1, LACTB, RGMA	SQRDL; SQOR, ULK3, SCAMP5
16	LPCAT2, BAIAP3, SULT1A1, NECAB2	COG7, LCMT1, NAE1, ITGAM, SLC9A3R2
17	ASPA, C1QBP, TRPV2, C17orf59; BORCS6, SHMT1, WBP2, TRIM25, FDXR, ACSF2, SEPT9, SPATA20	CAMKK1, TXNDC17, VAT1, DHRS11, SEPT4, GHDC, FLOT2, ACACA, AARSD1; PTGES3L-AARSD1, ACTG1
18		LMAN1
19	PLIN4, LONP1, ATP13A1, PEPD, ALDH16A1	SH3GL1, BRD4, MAP1S, MEGF8, UBE2M
20	CPNE1, TGM2, ITPA	PLCG1, AHCY, PHACTR3, ARFGAP1, RPS21, RPN2, GSS
21	JAM2, PCP4	
22	ARVCF, APOL2, PACSIN2, SYN3	AIFM3